Article:
Lai, Y. orcid.org/0000-0002-9987-0975, Wang, X., Rockett, T.B.O. et al. (2 more authors) (2022) Investigation into wind effects on fire spread on inclined wooden rods by multi-spectrum and schlieren imaging. Fire Safety Journal, 127. 103513. ISSN 0379-7112

https://doi.org/10.1016/j.firesaf.2021.103513

Investigation into wind effects on fire spread on inclined wooden rods by multi-spectrum and schlieren imaging

Yufeng Lai [1,a], Xiao Wang [2,b], Thomas B. O. Rockett [3,a], Jon R. Willmott [4,a], and Yang Zhang [5,b*]

[1]y.lai@sheffield.ac.uk

[2]xwang42@sheffield.ac.uk

[3]t.b.rockett@sheffield.ac.uk

[4]j.r.willmott@sheffield.ac.uk

[5*]yz100@sheffield.ac.uk

[a]*Department of Electronic and Electrical Engineering, The University of Sheffield, Portobello Centre, Sheffield, S1 4ET, United Kingdom*

[b] *Department of Mechanical Engineering, The University of Sheffield, Sir Frederick Mappin Building, Sheffield, S1 3JD, United Kingdom.*

Abstract

A combined imaging system that can monitor the visible flame, invisible hot flow, flame temperature and surface temperature was developed to investigate the combustion of wooden rods inclined at 30 degrees under forced air flow. A micro wind tunnel is designed to generate the forced air flow that is at an angle with the fire rod. It is found that a low-speed air flow can enhance the combustion of the burning lifetime and charring rate, while a high wind speed can decrease the intensity of combustion. There were three aspects that were found to influence the burning and spreading of the fire: 1. The effect of flame temperature; 2. The temperature change of the wooden surface; 3. The effect of the flow field around the burning rods, particularly for the flow field underneath the rod surface. The statistics and visualisation have enhanced the understanding of the mechanisms of wood combustion in a forced air flow. The developed imaging system is beneficial for monitoring the combustion process because it can monitor the flame temperature, wood surface temperature and visualise the invisible hot combustion products simultaneously.

Keywords: wood combustion; heat convection; underneath hot gas parcel; pyrolysis; gas-phase combustion

1. Introduction

The wood burning behaviour in still air has been extensively studied in the aspects of burning rate[1], [2], aerodynamics[3], [4] flame dynamics[5], and radiation[6] and remarkable progress has been achieved [7]. The burning in still air conditions is easy to control, due to the burning being solely buoyancy-driven. However, a fire disaster mainly occurs with the involvement of wind flow, both natural and fire induced. The study becomes much more complicated with the presence of wind, as the involvement of wind flow significantly changes the flow field, flame morphological characteristics, mechanisms of heat transfer and more[7]. The forced air flow, which mainly influences the burning behaviour, is attributed to the horizontal momentum, that is generated by the flow, counteracting the vertical buoyancy that is generated by the fire[8].

The effects of the forced air flow are complicated and involved various aspects. Burning rate is one of the basic parameters that represent the burning behaviour under forced air flow; therefore, it has been extensively studied. Welker et al. [9] found that the burning rate of methanol fire decreased with the increasing wind speed. The trend of the burning rate is similarly found in the research of Apte et al. [9], Saito et al.[10] and Carvel et al.[11] as well. However, with a more detailed experimental study, Woods and Kostiuk [12] found the change of burning rate depends on the size of the square pool, which could show monotonic increase, constant, or non-monotonic response. In the study of McAllister et al. [13], the non-monotonic change of burning rate with increasing wind speed had been found from the different design of wood cribs. In addition, from the works of Hu et al. [14], it is also found there were turning points of wind speed inside various sizes of the pool, in which the monotonicity of burning rate changes.

The geometry of the flame can also be significantly affected by cross wind. Lin et al. [8] had studied the behaviour of pool fire on an inclined surface under a cross-wind, concluding that the flame height decreases with an increasing wind speed, while a larger inclination angle increases the flame height. Concerning the flame tilt angle, it is wildly acknowledged that the tilt angle of the flame increases with increasing wind speed[14][15][16]. The changes of flame geometry under a cross-wind are mainly caused by the existence of the negative pressure zone generated by the wind[8].

Regarding the effects of the forced air flow on temperature, Himoto[17] used a series of thermocouples to read the temperature elevation at different heights and distances of a fire plume. Luan et al. [18] utilised an experimental wind tunnel to simulate the

effects of canyon cross-wind on the temperature distributions inside volumes of smoke. They used thermocouples to read the smoke temperature inside the wind tunnel and found the temperature change had a general decrease with increasing wind speed. In the work of Salvagni et al.[15][16], thermography was used for building a temperature map of flame under various wind speeds. It was found that the temperature in the reaction region was increased with increasing wind speed due to the additional air mixing, while the temperature was decreased in the edge of the flame because of the higher heat loss rate.

In addition, the air flow field had been simulated by Computational Fluid Dynamics (CFD). In Eftekharian et al.'s work [19], the computed results indicated that the cross-wind acted as a driving force to accelerate the flow and cause the wind enhancement downstream of the fire source. From the simulation results of Zhu et al.'s [20], it is found that the flow fields near the fuel pan varied from horizontal surface to inclined surface.

Many researchers focused on the wind effects on the geometry flame, burning rate, and mass loss, which are the general properties of wood combustion. Others studied the flow field change under forced air flow by CFD simulation. However, according to the literature reviews, studies concerning forced air flow mainly focused on the cross-wind while there are few publications that focused on how the air flow, which is parallel to the plane of fire propagation, influences the fire spread along the wood surface. The surface temperature of the wood surface under forced air flow has not been studied, yet it is an important parameter. The challenge can be considered that the invasive temperature measurement devices are difficult to apply due to the high temperature at the burning zone and the disturbance produced by the installation of devices. More importantly, invasive devices such as thermocouple are hard to read the precise temperature in the gas-phase since the heat would radiate much faster than its voltage changes. In addition, the flow field, especially the flow layer underneath the wood, was found to be a crucial factor in sustaining burning and spreading the fire, from Lai et al.'s work under the still air condition[21].There is no publication that visualises the hot flow layers under the wind condition. In our work, we developed a novel imaging system, which synchronised the visible, schlieren and thermal images with using the techniques of the temperature measurement by thermal imaging and two-colour method, for studying the effects of forced air flow on the fire spread on a single wooden rod. The use of single element fuel is convenient for experimental control, in addition, a clear visualisation of the hot gas layer underneath the wooden rod is achievable by using this simple setup. The samples in this

study were fixed at 30 degrees inclination, for maximising the fire spread phenomenon[21] [22]. In this study, a micro wind tunnel was designed for generating the forced air flow in the horizontal direction. Such scale of wind generator is suitable for the small samples used in this study with the advantages of a low cost and convenient optical access. The air flow direction was chosen for investigating the wind effects, both on the cross-section and along the rods, to better simulate reality. The non-invasive temperature measurement is suitable for the study of wood combustion as the temperature can be evaluated non-intrusively. The two-colour method is suitable for estimating the soot flame temperature and the thermal imaging is adequate for measuring the burning surface temperature. With the help of the schlieren imaging system, the flow field around the burning wood, that plays an important role in the combustion process, can be visualised. The mechanisms of forced air flow effects on fire spread can then be studied by synchronising the different images.

2. Experiment setup and methodology

In this study, the samples were made of oak wood and shaped into cylinders of 9.5 mm in diameter and 400 mm in length. All the samples were pre-dried in an electrical furnace, for 24 hours, at a temperature of 150 ^{o}C, to reach minimum water content.

The prepared samples were fixed at an inclination of 30 degrees by an adjustable holder, shown in Figure 1 (left). Each test was operated at 40 mm above the burner, to ensure repeatable burning conditions. The fuel of premixed methane-air was used to ignite the samples for 40 s. The wind generator was designed for the small samples consisting of an adjustable fan, with five different wind speed settings, a custom designed wind tunnel and five mesh layers, to provide a relatively homogenous air flow. The wind generator was set in front of the initial burning zone to provide the horizontal air flow in the same plane of the fire propagation, where the details of wind speed are presented in Table 1. The wind speed was measured at the end of the rods and 20 tests were made for the averaged measurements. The fan would be turned on once the burner turned off (the stage where self-sustained burning begins).

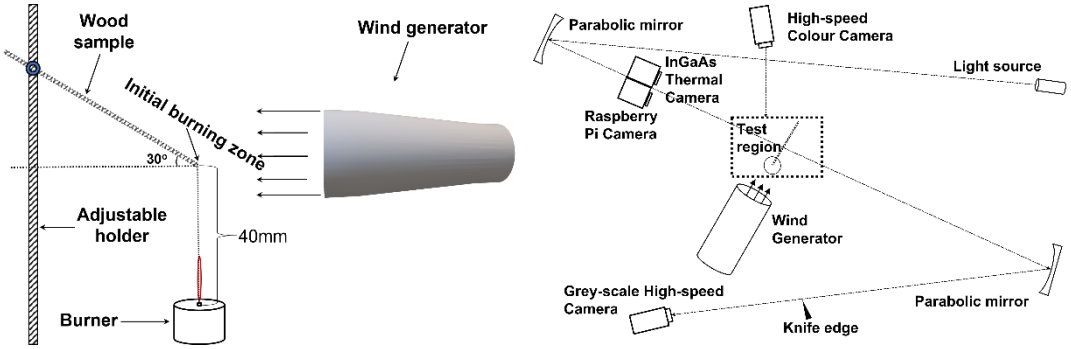

Figure 1 Left: schematic representation of the experimental set-up; right: the top view of the imaging system.

Premix fuel (L/min)		Ignition time (s)	Wind speed (m/s)	
Methane	0.34	40	Speed 0	0
			Speed 1	0.40
			Speed 2	0.49
Compressed air	0.9		Speed 3	0.62
			Speed 4	0.71
			Speed 5	0.77

Table 1 The parameters of experiment setup

The imaging system of this study comprised of multiple cameras, including:a grey-scale high-speed camera, which is used for a Z-type schlieren system; a CMOS high-speed colour camera, with an infrared (IR) cut-on filter, that is used to measure the soot flame temperature after a calibration process. An InGaAs thermal camera for wood surface temperature measuring, the camera could capture thermal images at a rate of 60 frames per second, with a cut-on filter to restrict its spectral sensitivity to 1550-1670 nm, to control the temperature range that the instrument was sensitive to. A raspberry pi camera, that could record 30 fps video, was used for capturing visible wavelength images. All the cameras were synchronised with each other and corrected with the same angle and position. The illustration of the imaging system is shown in Figure 1(right).

The flame temperature calculation is based on the two-colour temperature measurement technique[23], the fundamental principle of the two-colour method is based on Planck's law, after a specific calibration process, the temperature can be calculated by the intensity ratio of Red/Green channels[24]. Considering the soot emissivity fluctuates in different location of the flame[25], this technique has been approved as an efficient tool for measuring the soot temperature[26][27] since it could avoid the inaccurate emissivity estimation. Therefore, the flame temperature can be estimated by the soot temperature since the wood flame can be considered as a uniform distribution of a high concentration of soot particles[28][29]. The high-speed colour camera is able to measure the

temperature from 853ºC to 1873ºC according to dynamic range of the camera and background noise, the results would be built into colour map combined with temperature distributions, the results of averaged temperature were introduced as well; The wood surface temperature measurement is based on the calibration to a blackbody radiator which follows Planck's law. For a narrow band thermal imaging system, the most popular method for the calibration is based on the Sakuma Hattori model[30]. In this study, the InGaAs camera was calibrated with a fixed 16 ms exposure time to measure the wooden surface temperatures in the range 250-750 ºC. The imperfection of the results can be quantified by using the difference between the calculated temperature and the furnace temperature, which is shown in Fig.2. It is found that the residuals of two-colour technique were under 1% of temperature in Kelvin while the measured errors of thermal imaging technique were under 2% of temperature. The uncertainly of the measuring results can be caused by many factors, including the spectral emissivity, the radiometry calibration process, the curve fitting, the optical transmission of the device and the noise of this imaging system. However, the residuals of temperature performed fairly good in this temperature range.

The burning lifetime and charring rate were measured from the visible images. The burning lifetime was measured from the start of the sustained burning to the time point that all the visible flame disappeared. The charring rate was measured by the increase of the blackened length from the beginning of the self-sustained burning to 20 s of self-sustained burning. All the cases have been repeated 10 times to ensure repeatability. The burning lifetime and charring rate were averaged and shown their maximum and minimum residuals. Considering the burning under the wind speed 1 and 2 were more likely to keep self-sustaining, and in most cases the wood kept burning until the flame propagated to the end of the rods, which occurred after about 300 s. Therefore, the results only show the minimum burning lifetime in these two groups, which represent the exceptional cases that extinguished before becoming burned out along the whole rod. The samples were selected from the real natural wood rod which has a complicated and inhomogeneous internal structure [31] which resulted in the deviation from the results, the deviation of these experiments are natural and acceptable based on the repeatability of experiments.

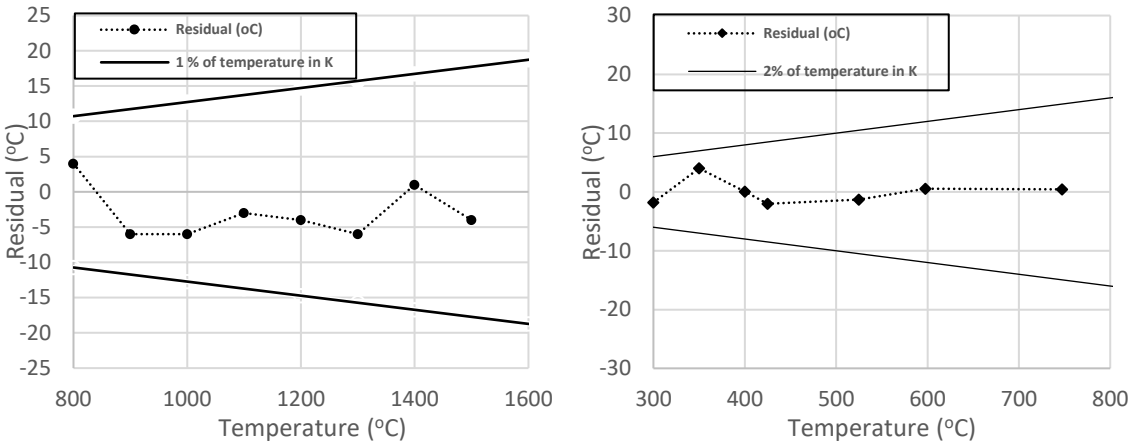

Figure 2 The residual of measured temperature against the blackbody temperature. Left: two-colour method; right: thermal imaging method.

3. Results and Discussion

Visible images captured by the raspberry pi camera are presented in Fig.3 under different wind speeds at 10s and 20s for illustrating a general trend of burning status. With the increasing wind speed, the flame had a considerable attachment phenomenon; the flame was enfolded along the wooden rod under wind speed 1 and speed 2. The appearance of the flame indicates that gas-phase combustion occurred[32], the larger size of the flame thus means stronger pyrolysis may have occurred.. As the flame appeared on both sides of the rod under wind speed 1 and 2, there were larger areas under thermal pyrolysis in these two cases. When the wind speed increased to speed 3, the whole flame attached to the bottom side of the wood surface. Moreover, the flame size and the intensity of image had significantly decreased when the wind speed increased to speed 4 and 5, which signified the gas-phase combustion became weak in these wind conditions. After 20 s of self-sustained burning, the flame was weakened and dimmed under wind speed 4 and 5, shown in the second row of Fig.3.

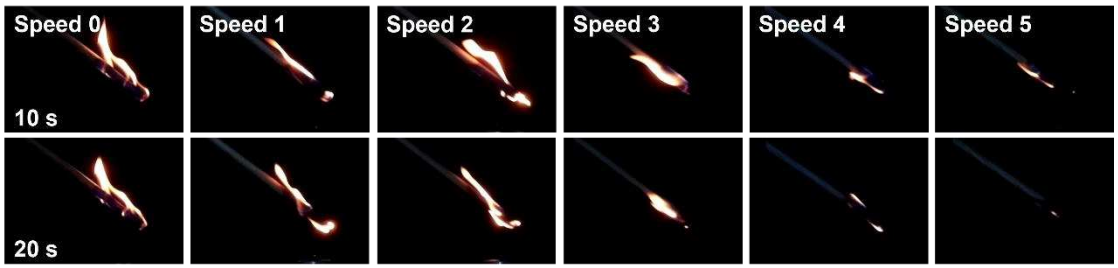

Figure 3 The direct images of self-sustained burning at 10 s and 20 s and different wind speeds.

The averaged burning lifetime from the beginning of self-sustained burning and the charring rate at the first 20 s are shown in Fig.4 with the maximum and minimum values. Combined with the results of the burning lifetime and the charring rate, the burning at 30 degrees surface was significantly enhanced when the wind speed 1 or 2 was involved, in both the intensity of burning and the fire propagation. In Fig.3, it can be seen the enhanced burning was attributed to the enfolded flame and the potential hot gas flow on both the topside and underneath of the rods, which could enhance the perpendicular combustion and longitudinal propagation respectively. With an increasing wind speed, although the intensity of flame was decreased, the burning front moved faster than the group without wind, due to the increased preheating underneath the rod. In the meantime, the stronger cooling under the higher wind speed and the insufficient combustion in the lateral direction resulted in a shorter burning lifetime under these air flow conditions.

In order to analyse this phenomenon, the effects of the forced air flow will be discussed in three main aspects: 1) The effects of flame temperature; 2) The temperature change of the wooden surface; 3) The effects of the flow field around the burning rods, particularly for the field underneath the rods surface. Through temperature measurements and visualisation, the phenomena can be quantified and analysed further.

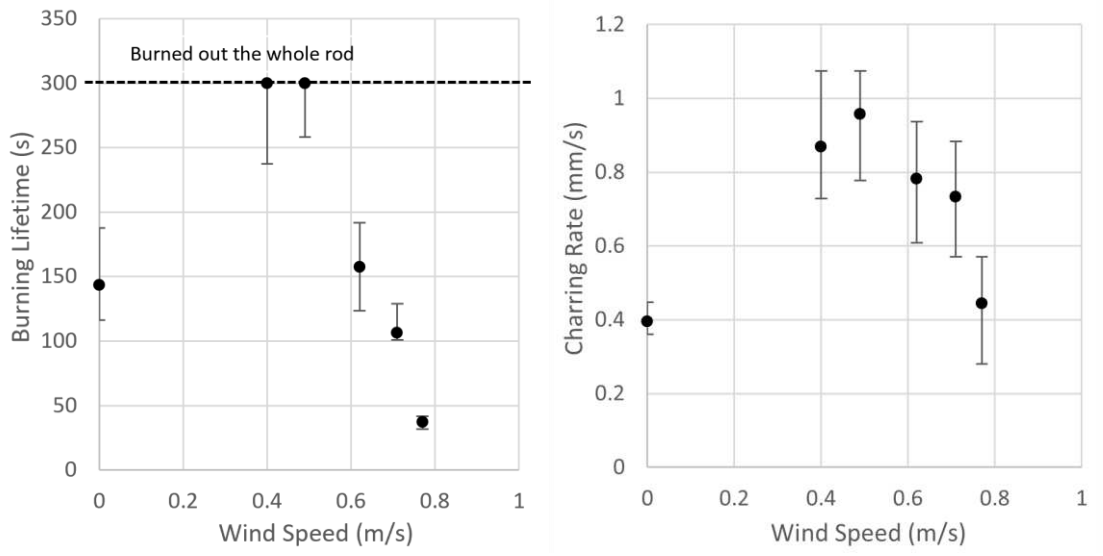

Figure 4 The averaged burning lifetime (left) and charring rate (right) against different air flow settings.

3.1. The effect of flame temperature

The wood flame may be considered as an uniform distribution of a high concentration of soot particles[28][29], therefore, the two colour method can be a suitable tool for estimating the flame temperature by measuring the soot temperature. Fig.5 presents the results of the flame temperature calculation at 10 s self-sustained burning under different wind conditions, for direct image (left), and temperature colour map (right). At the meantime, Fig.6 shows the mean temperature and standard deviation at this time point against wind speed.

It is found that the mean flame temperature is around 1610 ºC under the still air condition. It is worth noting that the average flame temperature slightly increased when the air flow was slow, then decreased with the higher velocity of wind speed and dropped quickly when the wind speed increased to 0.71 m/s. From the standard deviation results, it is found the flame temperature fluctuated stronger when the air flow was involved, and generally increased with the higher wind speed. Combined with the colour map in Fig.5, the conclusion can be derived that the deviation in low wind speed was attributed to the appearance of high temperature zone, while the large deviations under high wind speed were because there were more areas showed low temperature in these cases.

Regard to the temperature increase under low wind speed, the reason for the phenomenon is attributed to the increased oxygen supply. Another reason for this phenomenon is that the thermal pyrolysis rate is higher under low wind speed. According to the surface temperature results which would be shown in Section 3.2, the surface temperature excessed 300 ºC in the most region under wind speed 1 and 2, of which temperature was strongly agreed by other researchers representing the onset of rapid pyrolysis[32][33]. With the help of the high rate of thermal pyrolysis under wind speed 1 and 2, the reactions are more likely in the gas-phase combustion than the solid-phase oxidation, more flammable gases combined with larger oxygen supply made the flame temperature higher. In the meantime, low char residues under this temperature range [34] indicated the vapour would be easier to escape. In addition, the rapid exothermic reactions in these two cases enables faster de-moisturization, thus gives rise to higher temperatures. Besides, the cooler part is due to the increased convective heat loss to the surrounding cold air.

In contrast, the flame temperature is lower in the cases at speed 4 and 5. This phenomenon is attributed to the high rate of solid-phase oxidation, as the surface temperature decreased rapidly under the high wind speed, the thermal pyrolysis tends to be slower

under the temperature, lower than 300 ºC [32] [33], the wood temperature under different wind speed were measured by thermal imaging and shown in section 3.2 later. The pyrolysis rate tended to be less due to flame heat feedback is less under the high wind speed cases. In addition, the pyrolysis favoured producing solid products, like the carbon char [34]. The fewer combustible gases products under these cases made the flame become concentrated in a low volume zone and have a lower temperature. Another reason for increased heat loss was that the high wind speed increased the convective heat transfer between the flame and the cold air.

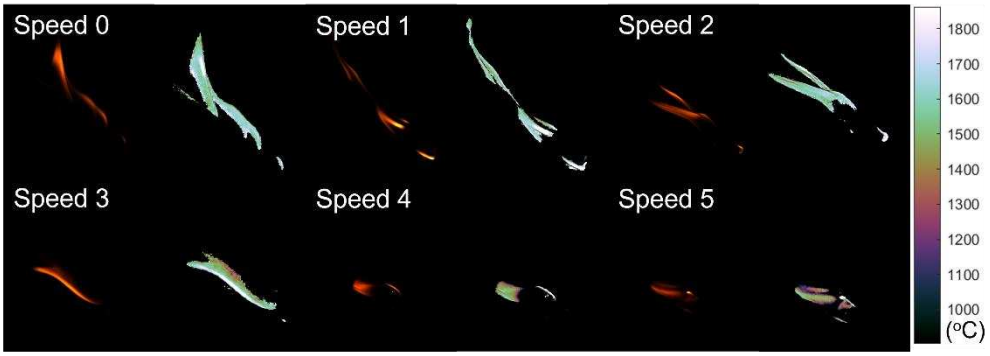

Figure 5 The actual flame and flame temperature colour map at 10 s self-sustained burning with different speed of air flow. Left: the actual flame; right: the temperature colour map.

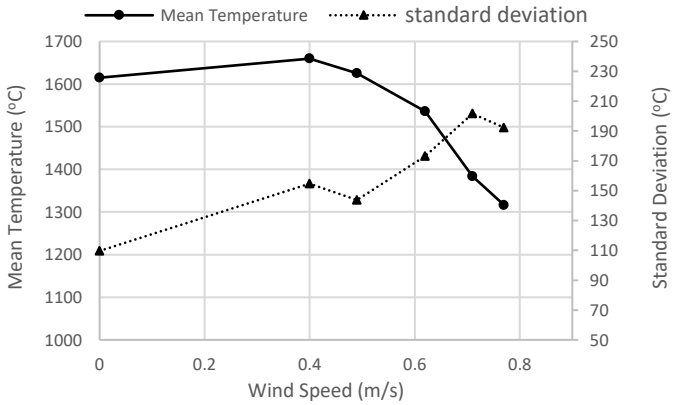

Figure 6 The mean temperature and standard deviation at 10 s self-sustained burning against different speed of air flow.

The flame temperature was averaged in each frame and compared to the results at different air flow speed, which is shown in Fig.7.It is found that averaged flame temperature slightly increased under wind speed 1 and 2 compared to the still air group. Further, the flame temperature started to decrease when the wind speed increased to speed 3 and dropped rapidly when the speed increased to 4 and 5. In the former case, the lower speed of wind increased the flame attachment and made the flame enfolded around both sides of the rod. The larger the area involved in the heat pyrolysis, the more combustible gases that were produced from the pyrolysis progress, which resulted in a higher intensity of combustion. In addition, the larger area enfolding the burning rod means there was

less area contacted directly with the surrounding cold air in the cases of speed 1 and 2, resulting in decreased heat loss of the flame. In contrast, in the high wind speed cases, the flame mainly appeared on the bottom side of the rods. According to the study of Tang et al.[35], the cross wind changed the flame intermittency distribution, and the flame length increased under high wind speed. This would increase the area contacted directly with the cold air, as a result, the flame temperature decreased with the higher air flow speed.

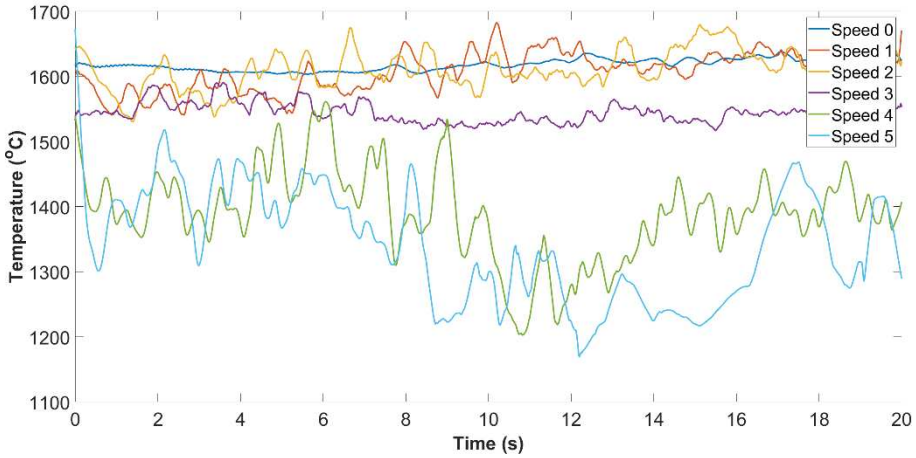

Figure 7 The time-dependant averaged flame temperature under different air flow speeds during the 20 s.

3.2. The effect of surface temperature

From the direct images in Fig.3, it is found there was observably lengthwise cooling starting from the rod end under higher velocity of wind speed. In order to determine the differences between cases quantitatively, the surface temperature of the surface at 10 s was calculated and is shown in Fig.8. It can be seen that the rods under still air/low wind speed conditions remained at a high temperature at 10 s, and the high temperature zone was concentrated at the bottom end of the rods, indicating these areas were under rapid thermal pyrolysis. In contrast, the high wind speed cases had significant cooling after 10 s self-sustained burning, the cooling started from the topside of rod to the underneath of the rod. Under wind speed 5, most areas on the topside had cooled under 300 °C, which means the rapid thermal pyrolysis has stopped on these areas [36], [37].

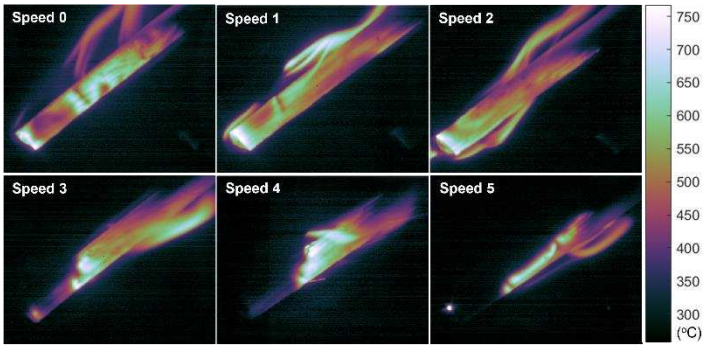

Figure 8 The surface temperature map of 10 s self-sustained burning with different speeds of air flow.

Fig.9 illustrates the region of interest (ROI) for the following investigation. The first point (point 0) is set at the very edge of the rod end representing the impact point (where a high volume of heat is concentrated during the ignition). Point 1 locates on the boundary of the impact point area. And point 2 and 3 represents the areas adjacent to the high-temperature zone. The distance between each point is 3 mm.

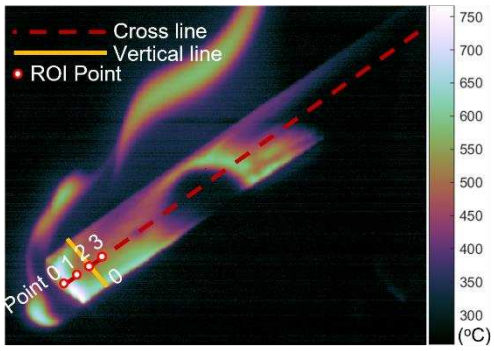

Figure 9 The illustration of the region of interest (ROI).

The Fig.10 presents the temperature change during the first 20 s of self-sustained burning at point 0 (indicates the impact point) and point 2 (adjacent to impact point) under different wind conditions. It is found that the temperature of the still air case remained high during this period at point 0, while it decreased slowly at point 2, due to the natural cooling. It is worth noting that under the slow wind condition (speed 1 and 2), the surface temperature slightly increased over time. The results indicated the surface under low velocity of air flow remained in high temperature over the time by increasing the convection heat transfer along the wood, resulted in a longer period of rapid pyrolysis and a longer burning lifetime.

In contrast, both the points (0 and 2) temperature in the cases under wind speed 3, 4 and 5 had dramatically dropped during this period. It should be highlighted that the temperature of point 2 did not dramatically drop at the beginning but slightly later after the

wind conditions involved. In addition, it can be observed that the time for the temperature reduction were different under wind speed 3, 4 and 5. The rod under higher wind speed cooled earlier.

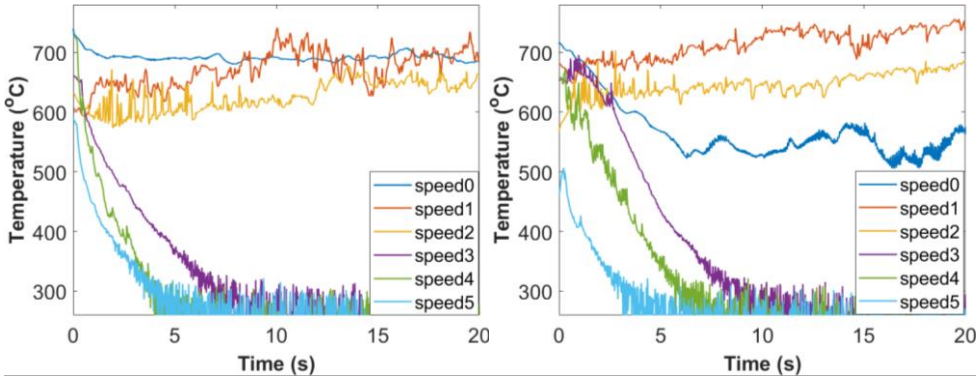

Figure 10 The first 20 s from the self-sustained burning temperature at point 0 (left) and point 2 (right) with different wind speed.

In order to deduce the difference between the cooling under the high wind speed groups, the temperature at four points along the rod against time is presented in Fig.11. For the reason that the cases of speed 1 and 2 did not present a significant lengthwise cooling at the first 20 s, the figure only showed the temperature evolutions of test sets at speed 3, 4, 5 and the still air conditions. From the results of the speed 0 case, all four points had a slow temperature decrease from the beginning of the self-sustained burning. The temperatures at point 0 and 1 without forced air flow decreased more slowly than those at point 2 and 3, which was due to the high concentration of combustible gases around this area and remained at high-intensity combustion.

It can be seen from the figures, the fast cooling of point 2 and 3 did not start from the beginning but a few seconds later under the high speed of the wind, the red-dotted line is used to indicate this period. The temperature of point 0 and 1 had a high value when the self-sustained burning began. Then, after the involvement of forced air flow, the temperature of these two points decreased immediately.

Instead, the temperature at point 2 and 3 increased at the beginning and then kept the high temperature before the fast temperature drop. This is for two reasons: firstly, the high volume of heat concentrated at the impact point during the ignition, the heat was brought towards the rods at the beginning by the air flow and the temperature remained high; secondly, there was a high concentration of combustible gases near the impact point, which was demonstrated in previous work[21], the blowing flow could bring the gas-phase fuel in addition with the oxygen supply to the unburned wood, which helped enhance the combustion at the beginning. The cooling reduces the high temperature zone. In addition, the time point when the temperature dropped rapidly was

affected by the wind speed. Cooling will occur earlier at higher wind speed. Earlier onset of fast cooling signifies that the high-volume heat in the impact point was cooled down faster under the condition of high wind speed. In terms of the cooling rate, it is clearly shown that the temperature reduced faster under the high wind speed. The high wind speed could significantly increase the convective heat loss, which then resulted in the increasing heat transfer coefficient.

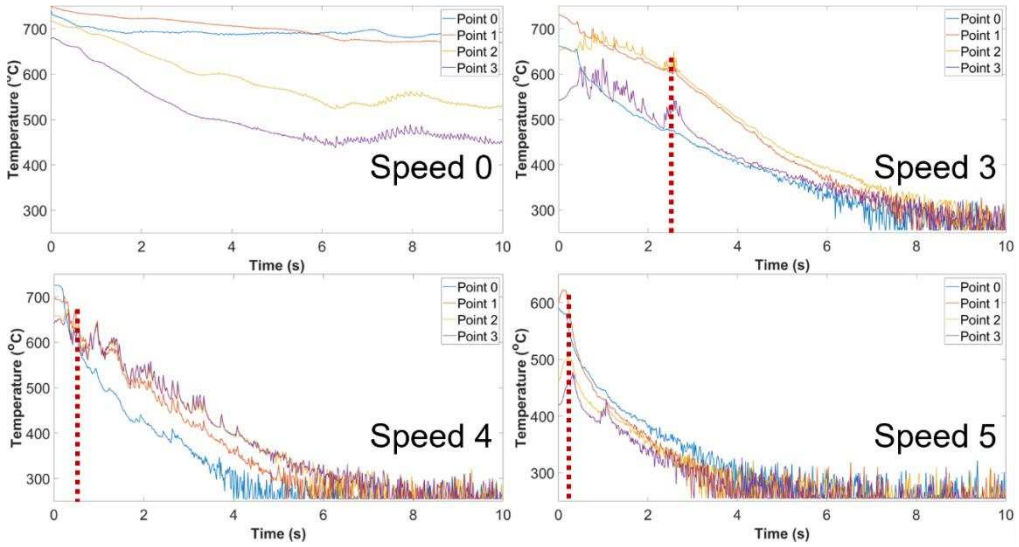

Figure 11 The first 10s from the self-sustained burning temperature at different positions with wind speed set 0, 3, 4 and 5.

The fire propagation on the wood surface was in two directions: longitudinal combustion and perpendicular combustion. The longitudinal preheating was shown to be the critical factor of the burning on the wood surface under the piloted ignition[21] [38] [39]. On the other side, although the perpendicular combustion showed insignificant impact on the fire propagation, it helped the sustaining of burning.

To deduce the effects of the forced air flow on the perpendicular combustion proceeded, the vertical line, which is demonstrated in Fig.8 was set for analysing the perpendicular direction temperature change. Fig.12 presents the vertical line temperature changed in the period of the first 20 s under different wind speeds. It can be seen that in still air, the high temperature concentrated in the underside and decreased slowly with time, representing the underside hot gas parcel and the heat transfer from the bottom to top. The top side temperature remained at a high level, this is because the flame kept heating the topside surface and the heat flux continuedly transfers from the bottom to the top, due to the effect of buoyancy.

With regard to the cases under the forced flow, in the cases of wind speed 1 and 2, the long length from underneath the wooden rod remained at a high temperature in the first 20 s, the combustion of the whole surface was distinctly enhanced under these conditions.

The temperature enhancement came from three aspects: firstly, it is attributed to the enfolded flame in addition with the higher flame temperature; secondly, the continual combustible gases supply produced from the pyrolysis of the impact point and the oxygen supply; thirdly, the heated gas flow underneath the rod that is unseeable in the visible range could promote combustion.

Regarding the high wind speed cases, it is found the vertical line region extinguished after 10 s of self-sustained burning under these three conditions. It should be highlighted that the temperature in the bottom side decreased after the extinguishment of the top side. It is because the perpendicular combustion plays an important role for helping sustain the burning. In addition, with increasing the wind speed, the thickness of the high-temperature layer from the bottom side significantly decreased. The main reason for this phenomenon is because the flame and heated flow only attached underneath the rod, insignificant heating in the top side weakened the thickness wise combustion. Another reason is the forced flow prevented the upward heat transfer by affecting the hot gas flow direction. The thicker layer of char formed under high speed of the wind, the fast cooling of underneath surface results in a high rate of solid-phase oxidation; therefore, the heat transfer is decreased due to the prevention of char layer.

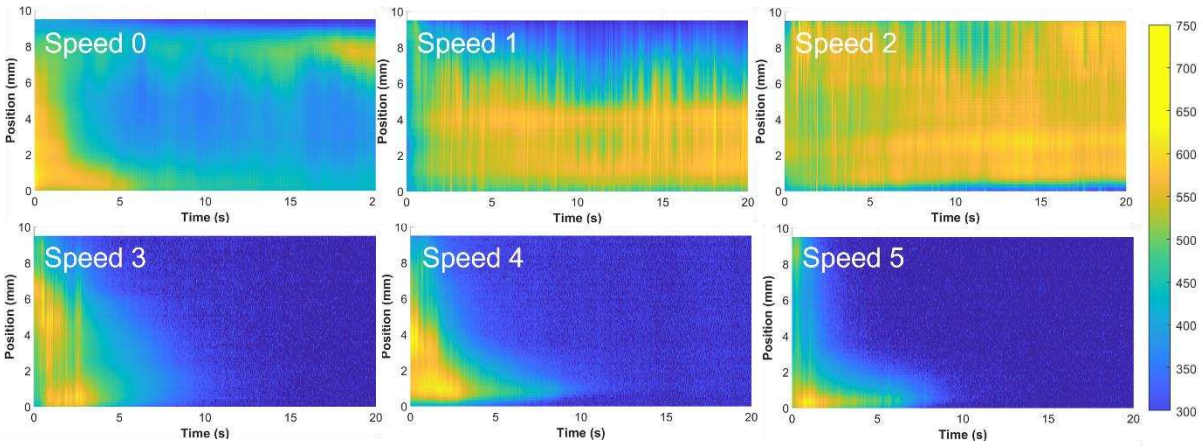

Figure 12 The vertical-line temperature map against time with different speed of air flow.

3.3. The effect of flow field

The surrounding hot gas flow is the crucial factor in sustaining burning and propagating flame, which had been demonstrated in previous work[4] [21]. The schlieren imaging technique had been applied for visualising and analysing the flow field along with the surface temperature map. Fig.13 shows the schlieren images matched with the surface temperature map at 10 s of self-sustained burning under the different wind conditions.

From the image of the still air condition, it can be seen that the hot gas flow appeared on both the underneath and the topside of the rod. Regarding the hot gas flow underneath the rod, it is attached closely to the bottom side of the rod. As well it can be clearly observed that the underneath hot gas parcel extended further than the pyrolysis front which is showed in the temperature map and preheated the adjacent unburned wood.

From the images of speed 1 and 2 cases, the flame under these two wind conditions blew into the top side of the wooden surface. It is found that the flame moved faster than the still air conditions. It should be noted that there was a large area where no flame appeared on the topside in these two cases. More importantly, even when there was no visible flame on the topside of this area, the surface remained at a high-temperature. The schlieren image could explain this interesting phenomenon. There was thick invisible hot gas flow attached, surrounding the no flame area surface both in the topside and the bottom. The underside flow layer represented there was heated from the underside, with the effect of the buoyancy, the heated flow could be transferred upward to heat deep within the wood surface. The attached hot flow layer on the top side indicates the pyrolysis proceeded and the gas-phase products formed the hot layer to maintain the temperature of the wood.

Meanwhile, with the increased wind speed, in the cases of speeds 3, 4 and 5, the flame tended to attach the bottom side of the rods due to the blowing of the high-speed wind, which indicates the gas-phase combustion only occurred on the bottom side.

It should be highlighted that the cooling of the surface in the high wind speed cases was along with the direction of wind and started from the top to the bottom. In the case of speed 3, the area near the end of the rod had completely extinguished while the temperature at the bottom side was still high enough for the rapid pyrolysis. The conclusion can be drawn from the images of speed 4 and 5 that the topside always extinguished before the underside. Combined with the schlieren images, it is found that the area where already cooled to extinguishment had no significant hot flow layer attached around the rod. This is attributed to the underside hot flow layer of the extinguished area blowing off and could not attach to the bottom side. No attached hot gas parcel underneath led to the conclusion that there was insufficient convective heating from the underside, in addition to the heat loss from the forced flow, which resulted in fast cooling of the deep rod surface. On the other side, there was no hot flow around the topside suggesting that the

pyrolysis ceased in that area. Neither hot gas flow from the combustion production nor the convective heating from underneath the wood in these areas showed a rapid cooling and extinguishment.

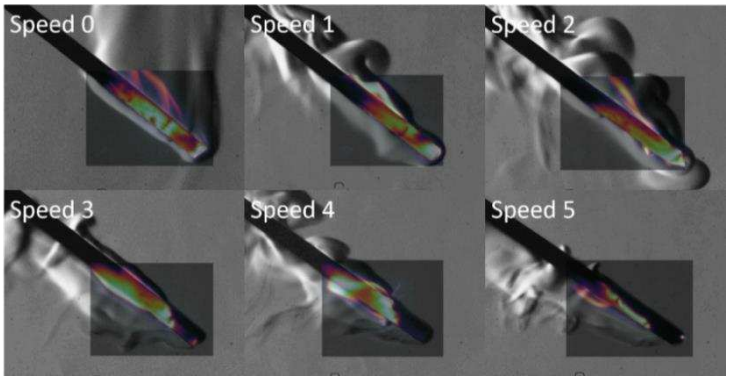

Figure 13 The synchronised schlieren image and temperature map at 10 s of self-sustained burning with different air flow speed.

In order to further study the effect of the forced air flow on the hot gas flow, the schlieren images under different wind speed set at 0s, 10s and 20s are shown in Fig.14. At the beginning of self-sustained burning, all the six cases had the thick hot flow parcel underneath. With forced air flow evolving, the heated flow was more likely to attach to the burning rod. Under wind speed 1 and 2, it covered both sides of the rod, while it was more likely to attach underneath the rod under wind speed 3, 4 and 5.

As seen, the preheating length was longer under the forced air flow where a large area was heated by the hot gas layer. However, by comparing the images between the cases with the forced flow, the hot gas layer was blown away from the underneath surface under the higher speed wind. There was no obvious layer of the underside hot flow under the wind speed 5. The hot flow under higher wind speed shows in a lower contrast than in the still air case reflecting the lower density of air. In contrast, the underside hot gas parcel remained in relatively high contrast in the images and could obviously be attached to the bottom surface in the cases of speeds 1 and 2. This is attributed to two aspects: the first is due to the heat transfer from the high-temperature area (impact point) that was increased by the air flow; the second is that the gas-phase combustion products increased with the enhancing burning.

After the 20 s of self-sustained burning, the hot gas flow in the cases of speeds 1 and 2 became larger in size and stronger in intensity. It indicates that the combustion was significantly enhanced under these wind conditions, and more combustion products were produced. The relationship might be found between the enhanced combustion and the increased gas-phase combustion products since the more combustion products produced, the more hot gas layer was supplied. With the help of the air flow, the gas-phase combustion products that came from the top side could be transferred into the adjacent underneath and continued to heat the deep

surface.

Comparatively, the high velocity of wind impeded the hot flow transfer upward. Therefore, the topside would be cooled quickly, resulting in less flammable gasses produced in the pyrolysis. This further led to the hot gas flow supply into the bottom side and resulted in the bottom side cooling afterwards.

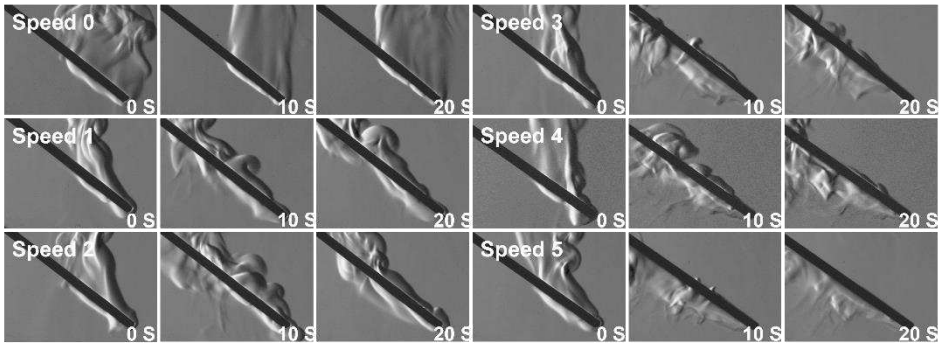

Figure 14 The illustration of underneath heated flow at 0s,10s and 20s under different air flow speed set.

Fig.15 illustrates the process of gas-phase products transfer. It is known that the hot gas flow came from the impact point and moved in two ways: the red line represents that the heated flow moved upward due to the buoyancy; the green line shows that the part of the upward hot flow moved along the sub- surface because of the Coanda Effect[40]. The upward hot flow could heat the deep layer of the surface and the flow in the longitude direction could preheat the adjacent wood. The black line indicates the gas-phase combustion products, which came from the deep surface of the rod, similarly moved in two ways: upward and along the rod. The part of heat flow that came from the burned surface could extend along the rod and preheat the same layer of the wood.

Under the low-speed wind, the movement of gas-phase products slightly tilts in the direction along with the wind. It can be seen that the underneath hot gas parcel (the green line) was blowing off the bottom surface slightly, while more gas-phase products were involved into the underneath (the black line) which is the reason why the underside hot flow was stronger under wind speed 1 and 2 in Fig.14. In addition, the hot gas flow moving upward (the red line) had a tilted angle with the wooden rod instead of the vertical direction. This would increase the fire propagation rate due to the faster heat transfer along the rod.

However, with the increased wind speed, the larger amount of the underside hot flow blew away from the bottom surface (the green line), the high velocity of wind made the hot flow unable to attach on the surface. Moreover, the upward moving hot flow (the red line) was significantly affected by the forced air flow and cannot be transferred upward effectively. As a result, a large area on the

topside cannot be heated, cooled fast, and more char formed while less flammable gases were produced as a consequence, as shown in the blue colour area in the third image. This is the reason that the high wind speed cases had a relatively higher charring rate than the no-wind group but a shorter burning lifetime. Another reason is the hot flow supply from the deep surface, due to the larger area fast cooled, there were less gas-phase combustion products supply into the underneath. As result, the underneath hot gas parcel became thinner with time.

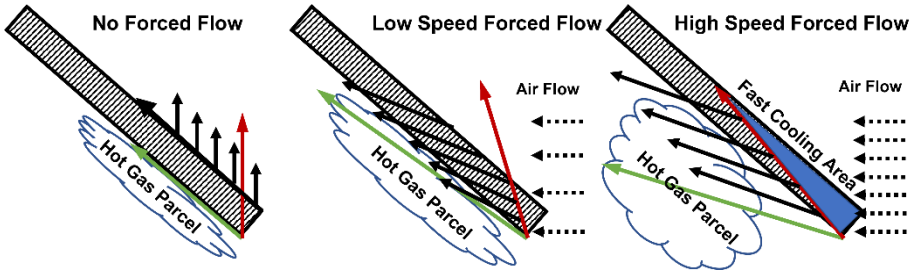

Figure 15 The illustration of the convective heat transfer and the supply of the hot gas flow underneath. Red line indicates the upward moving hot gas flow, black line indicates the moving direction of hot gas flow generated from deep surface.

4. Conclusion

Using the multiple camera imaging system and non-invasive temperature measurement, the influences of forced air flow on wooden rods fire spread were investigated. Generally, the combustion was enhanced when low-speed wind (speed 1 and 2) was applied. As the wind speed increased, the intensity of combustion was observed to decrease significantly. This phenomenon was attributed to three aspects: the flame temperature, the wooden surface temperature and the flow field around the burning rods. These three aspects interacted with each other and determined the intensity of burning and the ability of fire propagation jointly. The flame temperature was evaluated by the two-colour method. From the statistical results, it is found that the flame temperature slightly increased with the low wind speed while decreased under high wind speed conditions. This phenomenon was attributed to the flame geometry and the thermal pyrolysis rate which is determined by the surface temperature. From the surface temperature obtained from the thermal images, it is found that the low speed of forced air flow enhanced the surface temperature while the high wind speed significantly increased the surface cooling. The wooden surface temperature was influenced by both the flame geometry and the convective heat transfer which generated by the hot gas flow. With the help of schlieren visualisation, it is observed that the low speed air flow helped the convective heat transfer by

increasing the hot gas-phase products underneath the rod. The high speed flow was seen to impede the heat transfer upward, besides the dilution of the underneath hot gas layer. In addition, cooled wooden surface under the high-speed forced wind decreased the gas-phase products generation of the deep surface, further decreased the convective heat transfer from the heated gas flow.

Acknowledgements

The research work is partly supported by the Leverhulme International Academic Fellowship (IAF-2019-034).

References

[1] J. Zhao, H. Zhu, J. Zhang, H. Huang, and R. Yang, "Experimental study on the spread and burning behaviors of continuously discharge spill fires under different slopes," *J. Hazard. Mater.*, vol. 392, no. December 2019, p. 122352, 2020.

[2] H. C. Tran and R. H. White, "Burning rate of solid wood measured in a heat release rate calorimeter," *Fire Mater.*, vol. 16, no. 4, pp. 197–206, 1992.

[3] K. Hiroshi and Y. Taro, "Air entrainment and thermal radiation from heptane pool fires," *Fire Technol.*, vol. 24, no. 1, pp. 33–47, 1988.

[4] Y. Lai, H. Zhou, and Y. Zhang, "Experimental Investigation of the Fire Spread on Inclined Wooden Rods," pp. 1–6, 2019.

[5] B. J. McCaffrey, "Purely Buoyant Diffusion Flames (NBSIR 791910)," no. October, 1979.

[6] M. Muñoz, J. Arnaldos, J. Casal, and E. Planas, "Analysis of the geometric and radiative characteristics of hydrocarbon pool fires," *Combust. Flame*, vol. 139, no. 3, pp. 263–277, 2004.

[7] L. Hu, "A review of physics and correlations of pool fire behaviour in wind and future challenges," *Fire Saf. J.*, vol. 91, pp. 41–55, 2017.

[8] Y. Lin, L. Hu, X. Zhang, and Y. Chen, "Experimental study of pool fire behaviors with nearby inclined surface under cross flow," *Process Saf. Environ. Prot.*, vol. 148, pp. 93–103, 2021.

[9] J. R. Welker and C. M. Sliepcevich, "Burning rates and heat transfer from wind-blown flames," *Fire Technol.*, vol. 2, no. 3, pp. 211–218, 1966.

[10] N. Saito, "Experimental study on fire behavior in a wind tunnel with a reduced scale model," in *Proc. of the 2 nd Int. Conference of Safety in Road and Rail Tunnels*, 1995, pp. 303–310.

[11] R. O. Carvel, A. N. Beard, and P. W. Jowitt, “A Bayesian estimation of the effect of forced ventilation on a pool fire in a tunnel,” *Civ. Eng. Environ. Syst.*, vol. 18, no. 4, pp. 279–302, 2001.

[12] J. A. R. Woods, B. A. Fleck, and L. W. Kostiuk, “Effects of transverse air flow on burning rates of rectangular methanol pool fires,” *Combust. Flame*, vol. 146, no. 1–2, pp. 379–390, 2006.

[13] S. McAllister and M. Finney, “The Effect of Wind on Burning Rate of Wood Cribs,” *Fire Technol.*, vol. 52, no. 4, pp. 1035–1050, 2016.

[14] L. Hu, C. Kuang, X. Zhong, F. Ren, X. Zhang, and H. Ding, “An experimental study on burning rate and flame tilt of optical-thin heptane pool fires in cross flows,” *Proc. Combust. Inst.*, vol. 36, no. 2, pp. 3089–3096, 2017.

[15] R. G. Salvagni, M. L. S. Indrusiak, and F. R. Centeno, “Biodiesel oil pool fire under air crossflow conditions: Burning rate, flame geometric parameters and temperatures,” *Int. J. Heat Mass Transf.*, vol. 149, 2020.

[16] R. G. Salvagni, F. R. Centeno, and M. L. S. Indrusiak, “Burning rate, flame geometry and temperature of convection-controlled circular diesel oil pool fire under air crossflow conditions,” *J. Hazard. Mater.*, vol. 368, no. December 2018, pp. 560–568, 2019.

[17] K. Himoto, “Quantification of cross-wind effect on temperature elevation in the downwind region of fire sources,” *Fire Saf. J.*, vol. 106, no. January, pp. 114–123, 2019.

[18] D. Luan *et al.*, “Experimental investigation of smoke temperature and movement characteristics in tunnel fires with canyon cross wind,” *J. Wind Eng. Ind. Aerodyn.*, vol. 210, no. September 2020, p. 104531, 2021.

[19] E. Eftekharian, Y. He, K. C. S. Kwok, R. H. Ong, and J. Yuan, “Investigation of fire-driven cross-wind velocity enhancement,” *Int. J. Therm. Sci.*, vol. 141, no. March, pp. 84–95, 2019.

[20] P. Zhu, X. S. Wang, Y. P. He, C. F. Tao, and X. M. Ni, “Flame characteristics and burning rate of small pool fires under downslope and upslope oblique winds,” *Fuel*, vol. 184, pp. 725–734, 2016.

[21] Y. Lai, X. Wang, T. B. O. Rockett, J. R. Willmott, H. Zhou, and Y. Zhang, “The effect of preheating on fire propagation on inclined wood by multi-spectrum and schlieren visualisation,” *Fire Saf. J.*, vol. 118, 2020.

[22] Y. Wu, H. J. Xing, and G. Atkinson, “Interaction of " re plume with inclined surface,” vol. 35, pp. 391–403, 2000.

[23] H. C. Hottel and F. P. Broughton, “Determination of True Temperature and Total Radiation from Luminous Gas Flames,” *Ind. Eng. Chem. Anal. Ed.*, vol. 4, no. 16, pp. 166–175, 1932.

[24] M. M. Hossain, G. Lu, D. Sun, and Y. Yan, “Three-dimensional reconstruction of flame temperature and emissivity distribution using optical tomographic and two-colour pyrometric techniques,” *Meas. Sci. Technol.*, vol. 24, no. 7, p. 074010, 2013.

[25] G. De Falco, G. Moggia, M. Sirignano, M. Commodo, P. Minutolo, and A. D’Anna, “Exploring soot particle concentration and emissivity by transient thermocouples measurements in laminar partially premixed coflow flames,” *Energies*, vol. 10, no. 2, pp. 1–12, 2017.

[26] G. Lu, Y. Yan, G. Riley, and H. Chandr Bheemul, “Concurrent measurement of temperature and soot concentration of pulverized coal flames,” *IEEE Trans. Instrum. Meas.*, vol. 51, no. 5, pp. 990–995, 2002.

[27] H. C. Zhou *et al.*, “Experimental investigations on visualization of three-dimensional temperature distributions in a large-scale pulverized-

coal-fired boiler furnace," *Proc. Combust. Inst.*, vol. 30, no. 1, pp. 1699–1706, 2005.

[28] Gang Lu, Yong Yan, S. Cornwell, and G. Riley, "Temperature Profiling of Pulverised Coal Flames Using Multi-Colour Pyrometric and Digital Imaging Techniques," *2005 IEEE Instrumentationand Meas. Technol. Conf. Proc.*, vol. 3, no. 4, pp. 1658–1662, 2005.

[29] Z. W. Jiang, Z. X. Luo, and H. C. Zhou, "A simple measurement method of temperature and emissivity of coal-fired flames from visible radiation image and its application in a CFB boiler furnace," *Fuel*, vol. 88, no. 6, pp. 980–987, 2009.

[30] F. Sakuma and S. Hattori, "Establishing a practical temperature standard by using a narrow-band radiation thermometer with a silicon detector," 1983.

[31] V. K. R. Kodur and T. Z. Harmathy, *Handbook of Fire Protection Engineering*. 2016.

[32] A. I. Bartlett, R. M. Hadden, and L. A. Bisby, "A Review of Factors Affecting the Burning Behaviour of Wood for Application to Tall Timber Construction," *Fire Technol.*, vol. 55, no. 1, pp. 1–49, 2019.

[33] H. W. Emmons and A. Atreya, "The science of wood combustion Howard W Emmons and Arvind Atreya heat ' heat transfer fuel mass transfer," vol. 5, no. December, pp. 259–268, 1982.

[34] R. H. White and M. A. Dietenberger, "Wood Products: Thermal Degradation and Fire," *Encycl. Mater. Sci. Technol.*, pp. 9712–9716, 2001.

[35] F. Tang, L. Li, Q. Wang, and Q. Shi, "Effect of cross-wind on near-wall buoyant turbulent diffusion flame length and tilt," *Fuel*, vol. 186, pp. 350–357, 2016.

[36] D. Drysdale, *An introduction to fire dynamics*. John Wiley & Sons, 2011.

[37] C. Lautenberger, S. Sexton, and D. Rich, "Understanding long term low temperature ignition of wood," in *international symposium on fire investigation science and technology, College Park, MD, September*, 2014, pp. 22–24.

[38] R. O. Weber and N. J. De Mestre, "Flame Spread Measurements on Single Ponderosa Pine Needles: Effect of Sample Orientation and Concurrent External Flow," *Combust. Sci. Technol.*, vol. 70, no. 1–3, pp. 17–32, 1990.

[39] T. Hirano, S. E. Noreikis, and T. E. Waterman, "Measured velocity and temperature profiles near flames spreading over a thin combustible solid," *Combust. Flame*, vol. 23, no. 1, pp. 83–96, 1974.

[40] D. J. Tritton, *Physical fluid dynamics*. Springer Science & Business Media, 2012.